Paper presented at the

Sixth Topical Meeting on the
Technology of Fusion Energy

San Francisco, California
March 3-7, 1985

CONF-850310--77

DE85 010506

SURFACE EFFECTS ON SPUTTERED ATOMS AND THEIR ANGULAR AND ENERGY DEPENDENCE

Ahmed M. Hassanein
Fusion Power Program, Argonne National Laboratory
9700 South Cass Avenue, Argonne, Illinois 60439 U.S.A.
(312) 972-5889

Submitted April 1985

For publication in FUSION TECHNOLOGY

DISCLAIMER

*Work supported by the U.S. Department of Energy.

SURFACE EFFECTS ON SPUTTERED ATOMS AND THEIR ANGULAR AND ENERGY DEPENDENCE*

Ahmed M. Hassanein
Fusion Power Program, Argonne National Laboratory
9700 South Cass Avenue, Argonne, Illinois 60439 U.S.A.
(312) 972-5889

ABSTRACT

A comprehensive three-dimensional Monte Carlo computer code, Ion Transport in Materials and Compounds (ITMC), has been developed to study in detail the surface related phenomena that affect the amount of sputtered atoms and backscattered ions and their angular and energy dependence. A number of important factors that can significantly affect the sputtering behavior of a surface can be studied in detail, such as having different surface properties and composition than the bulk and synergistic effects due to surface segregation of alloys. These factors can be important in determining the lifetime of fusion reactor first walls and limiters. The ITMC Code is based on Monte Carlo methods to track down the path and the damage produced by charged particles as they slow down in solid metal surfaces or compounds. The major advantages of the ITMC code are its flexibility and ability to use and compare all existing models for energy losses, all known interatomic potentials, and to use different materials and compounds with different surface and bulk composition to allow for dynamic surface composition changes. There is good agreement between the code and available experimental results without using adjusting parameters for the energy losses mechanisms. The ITMC Code is highly optimized, very fast to run and easy to use.

I. INTRODUCTION

The behavior of energetic ions in solids has long been studied both theoretically and experimentally for many years. The theoretical understanding of atomic-displacement effects in solids requires a detailed analysis of the physical processes involved in slowing down the incident ions. Two major theoretical methods are used to describe ion transport in a solid, i.e., the analytical approach and the Monte Carlo simulation process. The analytical method is based on the transport theory approach with special simplifying assumptions in order to make the problem easy to solve. This approach is usually restricted to certain applications and special cases. The Monte Carlo method is based on computer simulation of the scattering process and the slowing down of the incident particles in target materials. This technique has been extensively applied to the simulation of ion transport and slowing down.[1-5] The increasing popularity and variety of Monte Carlo calculations in the literature is due to several factors. One of these factors is the capability to simulate trajectories in complex configurations such as film/substrate targets with different alloy compositions. Another factor is the variety of the processes that can be studied with fine details such as range calculations, sputtering and backscattering coefficients and their energy and angular distributions. However, an important factor is the availability of large digital computers and fast processors that can actually compete with other analytical methods.

In this paper the essential features of the Monte Carlo computer code ITMC are reviewed. A more detailed description of the Code and its capability are given in Ref. 6. The code can be used to study ion penetration and damage produced in solids for various ion-target combinations with target materials being single element or alloy. The alloy can have different surface and bulk compositions due to possible surface segregation effects. Ion and energy reflection coefficients as well as their angular and energy dependence can also be studied. Sputtered atoms, their energy and angular distribution, and the location inside the target from which they are sputtered can be calculated for each atom species of the target. The individual contribution of primary and secondary knock-on atoms to the total sputtering yield can also be evaluated for each atom species. Almost all the known interatomic potentials can be used to calculate the nuclear scattering cross sections. Switching from one potential to another at certain energies is easily done to study the effect of the interatomic potential on range, sputtering, and backscattering calculations. The influence of the inelastic

*Work supported by the U.S. Department of Energy.

energy loss on various calculations can be studied by using different models for the slowing down of particles in the target.

II. BASIC ASSUMPTIONS

In the Monte Carlo calculation, physical quantities such as ion penetration depth, backscattering and sputtering yields and their spatial, energy, and angular distributions are evaluated from the simulation of the scattering events occurring in a large number of simulated ion trajectories within the target. Thus, the accuracy in calculation depends on the number of trajectories used as well as how precisely the calculation simulates the actual complicated trajectories in the target. In the present calculation, like most Monte Carlo methods, the scattering process is simulated on the following major assumptions:

(1) the atoms are arranged randomly in the target, i.e., no lattice directional properties are considered;

(2) the collision between an incident ion and any target atom is binary with no influence of neighboring atoms; and

(3) the moving particle loses energy continuously to electrons while travelling between successive collisions at which nuclear losses occur.

III. CALCULATION PROCEDURE

A brief summary of some of the models used in the code is presented here. The formulations used for nuclear scattering and energy loss and the electronic stopping power are given below.

A. Nuclear Scattering

The universal differential scattering cross-section given by LSS theory is[7]

$$d\sigma = \pi a^2 \frac{f(t^{1/2})}{2\, t^{3/2}}\, dt \ , \qquad (1)$$

where

$$t^{1/2} = \varepsilon \sin(\theta/2) \ , \qquad (2)$$

$$\varepsilon = \text{reduced energy} = \frac{M_2}{(M_1 + M_2)} \frac{a}{Z_1 Z_2 e^2} E \ , \qquad (3)$$

and θ is the scattering angle in the center of mass system. M_1 and Z_2 are the atomic mass and number respectively for incident ion; subscript 2 is for target atom.

The screening parameter, a, can be given by:

Lindhard[7]

$$a = 0.8853\, a_o (Z_1^{2/3} + Z_2^{2/3})^{-1/2} \ , \qquad (4)$$

Firsov[8]

$$a = 0.8853\, a_o (Z_1^{1/2} + Z_2^{1/2})^{-2/3} \ , \qquad (5)$$

where $a_o = 0.529\text{Å}$ is the Bohr radius.

The universal scattering function $f(t^{1/2})$ can be written as [9]

$$f(t^{1/2}) = \lambda t^{1/2-m} \left[1 + (2\lambda t^{1-m})^q\right]^{-1/q} \ , \qquad (6)$$

where the coefficient λ, m, and q are fitting parameters adjusted for different interatomic potentials as shown in Table I. Although the extrapolation of this scattering function may not be accurate at low values of energy, the cross sections are only used on a relative basis. At low energies where the screening effect becomes more effective, the Born-Mayer (BM) potential is used. The scattering function for this potential is given as[10]

$$f(t^{1/2}) = 24\, t^{1/2} \ . \qquad (7a)$$

The energy below which this potential can be used is estimated to be[6]

$$E_o = 2.23\, Z_1 Z_2 e^2 \frac{(M_1 + M_2)}{M_2} a^2 \ . \qquad (7b)$$

A combination of any of the potentials shown in Table I and BM potential can be used in calculating the nuclear-scattering cross section. The total scattering cross section σ_T is then given by

$$\sigma_T = \int_{t_{min}^{1/2}}^{t_{max}^{1/2}} d\sigma \ , \qquad (8)$$

where

$$t_{max}^{1/2} = \varepsilon \sin\frac{\pi}{2} = \varepsilon \ , \qquad (9)$$

$$t_{min}^{1/2} = \varepsilon \sin\frac{\theta_{min}}{2} \ . \qquad (10)$$

The minimum angle of scattering θ_{min} can be determined from Eq. (8) assuming that

$$\sigma_T = \sum_j^{NT} N_j^{-2/3} \ , \qquad (11)$$

TABLE I

The Coefficients of the Universal Scattering Function[4,11]

Potential	λ	m	q
1. Thomas-Fermi-Sommerfeld (TFS)	1.7	0.311	0.588
2. Bohr (B)	2.37	0.103	0.570
3. Lenz-Jense (LJ)	2.92	0.191	0.512
4. Moliere (MOL)	3.07	0.216	0.530
5. Thomas-Fermi (TF)	1.309	0.333	0.667
6. Wilson (W)	3.35	0.2328	0.4445
7. Kalbitzer and Oetzmann (KO)	2.54	0.25	0.475

where N_j is the atom density of type j and NT is the total number of species in a polyatomic target. The scattering angle θ_i after collision (i) is determined from a uniform random number R_1 ($0 \leq R_1 \leq 1$), where

$$R_1 = \sigma(t^{1/2})/\sigma_T \ . \tag{12}$$

The numerical methods used in determining both θ_{min} and θ_i are highly optimized and very accurate and are described in detail in Ref. 6. The azimuthal scattering angle ϕ_i is determined from another uniform random number R_2 where

$$\phi_i = 2\pi R_2 \qquad (0 \leq R_2 \leq 1) \ . \tag{13}$$

The nuclear energy loss at each collision can then be calculated as

$$\Delta E_n = \frac{4M_1M_2}{(M_1 + M_2)^2} E \sin^2 \frac{\theta_i}{2} \ . \tag{14}$$

B. Electronic Energy Loss

Four different models for the electronic-stopping cross sections can be used to calculate the inelastic energy loss during particle slowing down. These models are Lindhard-stopping formula, Bethe-Block equation, Brice semi-empirical correlation, and Ziegler-fitting coefficients. The Lindhard formula is usually used in the low energy regime and the stopping power per unit length is given by

$$S_L = K_L E^{1/2} \ , \tag{15}$$

where

$$K_L = Z_1^{1/6} \left[\frac{0.0793 \ Z_1^{1/2} Z_2^{1/2} (A_1 + A_2)^{3/2}}{(Z_1^{2/3} + Z_2^{2/3})^{3/4} A_1^{3/2} A_1^{1/2}} \right] \ . \tag{16}$$

The Bethe equation is used for incident ion velocities $v > v_o Z_1^{2/3}$, where v_o is Bohr velocity. The stopping power is given by[1]

$$S_B = \frac{8\pi \ Z_1^2 \ e^4}{I_o \epsilon_B} \ln \epsilon_B \tag{17}$$

and

$$\epsilon_B = 4 \frac{m_e}{M_1} \frac{E}{Z_2 I_o} \ , \tag{18}$$

where $(Z_2 I_o)$ is the mean excitation energy and m_e is the electron mass. The mean ionization potential, I_o is given by[12]

$$I_o = \begin{cases} 12 + 7 \ Z_2^{-1} \text{ ev} & Z_2 < 13 \\ 9.76 + 58.5 \ Z_2^{-1.19} \text{ ev} & Z_2 \geq 13 \ . \end{cases} \tag{19}$$

The Brice[13] formula which contains three fitting parameters for each ion-target combination for a wide range of energy can also be used to calculate the electronic stopping. For light ions the Ziegler[14] fitting coefficients can also be used to calculate the electronic losses for a wide range of energy.

The motion of the incident particle between collisions is simulated as free flights of certain length, δ, where the particle loses energy due to electrons. The step length between collisions can be assumed either constant or proportional to the mean free path, i.e.,

$$\sigma = \sum_j^{NT} N_j^{-1/3} \tag{20}$$

or the step length can be calculated from a uniform random number R_3 as

$$\delta = - \sum_j^{NT} N_j^{-1/3} \ln R_3 \qquad (0 < R_3 \leq 1) \ . \tag{21}$$

Then the electronic energy loss ΔE_e is simply

$$\Delta E_e = \sum_j^{NT} N_j S_j \delta \ , \tag{22}$$

where S_j is the stopping power for atom species j.

In a fixed frame of reference, the direction cosines of the particle velocity vector must be calculated after each collision. Let $(\alpha_i,\beta_i,\gamma_i)$ be the direction cosine of the particle after the i-th collision. It can be easily shown that

$$\begin{bmatrix}\alpha_i\\ \beta_i\\ \gamma_i\end{bmatrix} = \begin{bmatrix}\alpha_{i-1}\\ \beta_{i-1}\\ \gamma_{i-1}\end{bmatrix} \cos\theta_i^* + \begin{bmatrix}-\beta_{i-1}\\ \alpha_{i-1}\\ 0\end{bmatrix} \frac{\sin\theta_i^* \cos\phi_i}{\sqrt{1-\gamma_{i-1}^2}} + \begin{bmatrix}-\alpha_{i-1}\gamma_{i-1}\\ -\alpha_{i-1}\beta_{i-1}\\ 1-\gamma_{i-1}^2\end{bmatrix} \frac{\sin\theta_i^* \sin\phi_i}{\sqrt{1-\gamma_{i-1}^2}}, \tag{23}$$

where θ_i^* is the scattering angle in the laboratory system, and is given by

$$\cos\theta_i^* = \frac{M_1 + M_j \cos\theta_i}{(M_1^2 + 2M_1M_j\cos\theta_i + M_j^2)^{1/2}}. \tag{24}$$

The position of the particle at the point of collision, i, is then given by

$$\begin{aligned} x_i &= x_{i-1} + \alpha_{i-1}\delta \\ y_i &= y_{i-1} + \beta_{i-1}\delta \\ z_i &= z_{i-1} + \gamma_{i-1}\delta \end{aligned} \tag{25}$$

IV. SIMULATION OF KNOCK-ON CASCADE AND SURFACE EFFECTS

For polyatomic targets prior to each collision, a random number is generated to decide the type of atom to be collided with. The probability of collision can be calculated assuming different cross-section models. It is assumed in this calculation that the probability of collision is proportional to the atomic density of the species. If any target atom (j) receives an energy $E^j = \Delta E_n > E_d^j$ (displacement energy of atom j) and also $E^j > E_b^j$ (binding energy of atom j), this atom will be set in motion with an energy $E^j = \Delta E_n - E_b^j$ and undergo similar scattering events as the incident particle and a cascade is generated. The recoiled atom in a cascade continues to move, losing its kinetic energy through both elastic and inelastic scattering, until its energy falls below a cut-off energy E_c^j (usually assumed equal to the surface binding energy E_s^j) or it leaves the surface as a sputtered atom. For an atom to leave the surface it has to overcome a surface barrier U. Two different models can be used to calculate U. The spherical model in which $U^j = E_s^j$, and the planar model which is used in this calculation, in which $U^j = E_s^j/\cos^2\theta_j$, where θ_j is the ejection angle of the sputtered atom j. In the ITMC code it is assumed that atoms trying unsuccessfully to leave the surface with energy $E^j < U^j$ but with enough energy $E^j > E_s^j$ will be reflected back into the target as if they were reborn again at the surface with incident energy equal to E^j and incident angle θ_j. These atoms will be followed until their energy falls below E_c or successfully leave the surface. However, if $E^j < U^j$ and $E^j < E_s^j$, these atoms are assumed to be buried in the surface layer.

V. RESULTS AND DISCUSSION

A. General Applications

Several examples demonstrating the validity of the code for various calculations using different ion-target combinations and compared with available experimental data and other known codes are given in Ref. 6. In this paper we examine some of the factors that can affect the sputtering yield due to surface and other related phenomena. One factor is the choice of potential to calculate the nuclear scattering cross section. There are several potentials developed during the past to describe the atomic interaction as shown in Table I. However, it is difficult to find an interatomic potential that describes such an interaction of any ion-target combination in all energy ranges. For example, it is known that TF potential overestimates the screening effect of the outer electrons especially at low energy, leading to a shorter range in target materials. Therefore, in these calculations the TF potential is used at higher energies and below certain energy, E_o [(Eq. (7b)], the BM potential is used. The effect of the choice of potential on the sputtering yield of silicon target bombarded by argon ions with different energies is shown in Fig. 1. The choice of argon-silicon combination is made because of the many available experimental data to compare with. The combination of TF + BM potentials yield the best sputtering result compared with two experimental sets of data, i.e., Kang et al.[15] and Southern et al.[16] At low ion energy of 1 keV the silicon sputtering yield predicted by MOL, LJ, and OK potentials is about factor of two to three lower than that given by TF + BM or the experimental data. Although there are no significant differences in the electronic and nuclear energy losses and the average number of primary recoil cascade among these potentials, the large difference in the sputtering yield

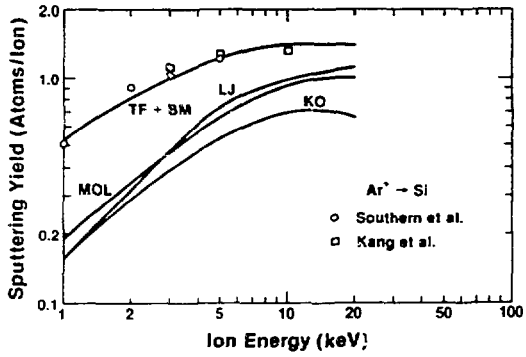

Fig. 1. Silicon sputtering yield as a function of argon ion energy for different interatomic potentials.

is mainly attributed to the fact that these cascades are generated near the surface in the case of TF + BM potential.[6] The ion range predicted by LJ potential is about 40% higher (at 10 keV) than TF potential with or without BM combination and is about a factor of two higher at lower energy (at 1 keV). The MOL and KO potentials yield a slightly higher range of 15 to 20% than the TF potential.

The silicon sputtering yield as a function of angle of incidence is shown in Fig. 2 for two different argon energies. The agreement is again very good between the code prediction using TF + BM potential and the experimental data.

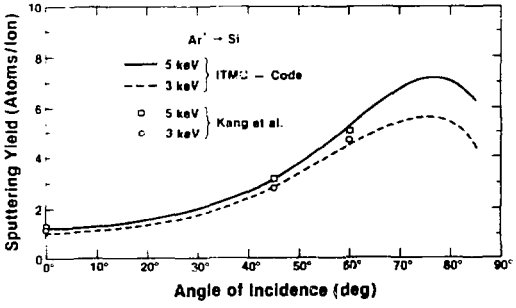

Fig. 2. Silicon sputtering yield as a function of argon ions angle of incidence.

The values of the displacement energy, binding energy, and surface energy can significantly affect the sputtering yield calculation. These values not only are scarcely known but also change with continuous ion bombardment as a result of damaged target structure. This fact should be considered in estimating the lifetime of a limiter or first wall of a fusion reactor especially when erosion and redeposition of target material are

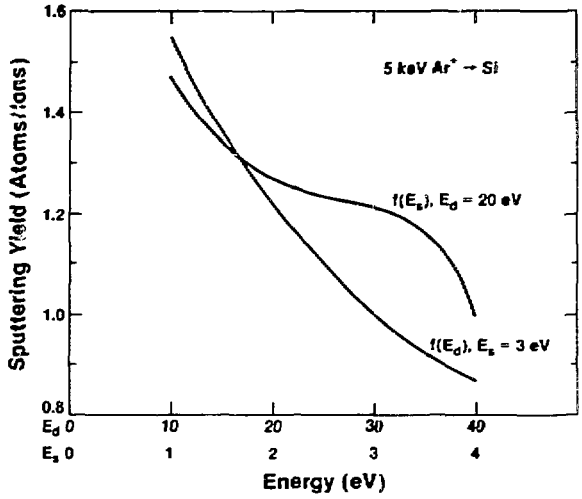

Fig. 3. Variations of sputtering yield with surface and displacement energies.

expected to occur. As an example, Fig. 3 shows the variation of the sputtering yield as a function of the surface and displacement energy for a fixed binding energy. The yield can easily vary by 30 to 40% with a slight variation in these energies. In ITMC code values, these energies need to be supplied and are not neglected as in other codes; no other adjusting parameters are used for the energy losses just to yield comparable results with the experiments. The values used for these energies are given in Ref. 6.

B. Surface Effects Due to Alloy Segration

A self-sustaining low-Z coatings for fusion applications involves the use of alloys in which thermal and radiation-related segregation that results in surface overlayers have been proposed.[17] These overlayers entirely consist of the low-Z component. Several alloys for candidate fusion reactor materials have been demonstrated as capable of producing such overlayers (e.g., Cu-Li, W-Be, and Va-Al).[18] These low-Z layers act as a plasma shield from the high-Z component of the alloy that could seriously affect plasma performance. One of these alloys is the vanadium-aluminum alloy (90% V-10% Al at.% bulk composition) in which the aluminum segregates and forms monolayers of pure aluminum on the surface. Figure 4 shows the vanadium self-sputtering yield for pure vanadium target and for vanadium-aluminum alloy with one and three monolayers of aluminum on the surface. The vanadium self-sputtering yield with one monolayer of aluminum on the surface is reduced by about a factor of two than that of pure vanadium. With three monolayers the self-sputtering is reduced by a factor of four at the low energy and by a factor of three at the high

energy shown in Fig. 4 and the self-sputtering yield does not exceed unity for energies up to 5 keV. The energy spectrum of the sputtered vanadium and aluminum atoms without and with aluminum on the surface for 1 keV incident vanadium ions are shown in Figs. 5 and 6, respectively. If there is no aluminum surface layer, the sputtering yield of aluminum is only about 14% of the total yield (the total yield is roughly equal to that of pure vanadium). On the other hand, when three monolayers of aluminum exist on the surface, the aluminum sputtering yield is about 75% of the total yield while the vanadium self-sputtering

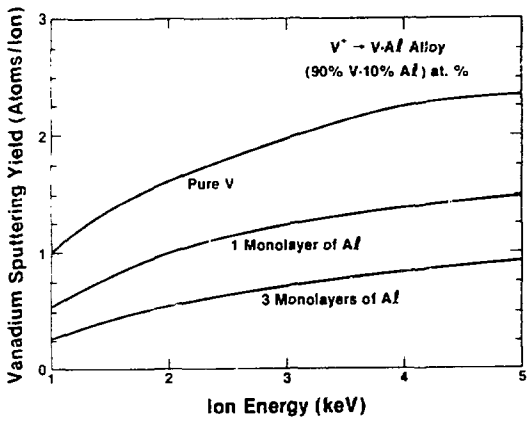

Fig. 4. Vanadium sputtering yield due to aluminum segration at the surface.

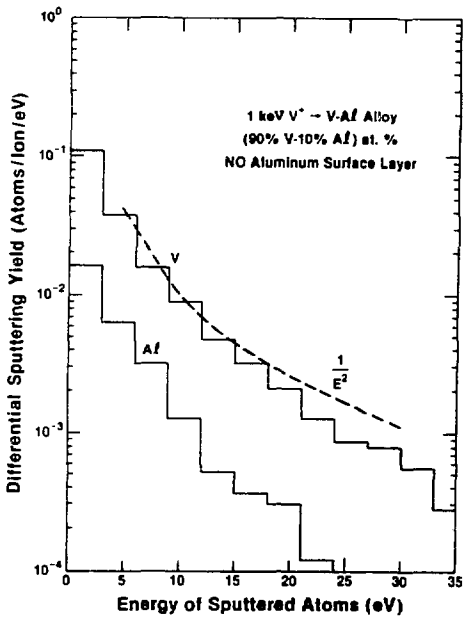

Fig. 5. Sputtered atom energy spectra with no aluminum on the surface.

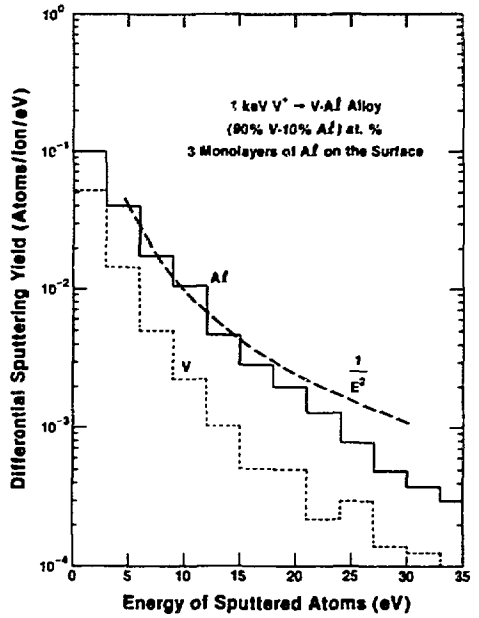

Fig. 6. Sputtered atoms energy spectra with three monolayers of aluminum on surface.

is only 25% of the total yield. In both cases the energy spectrum of the total sputtering atoms obeys the theoretical E^{-2} predictions fairly well.

VI. SUMMARY AND CONCLUSIONS

A comprehensive three-dimensional Monte Carlo computer code (ITMC) has been developed to study ion penetration and its related phenomena in single elements or alloys with different multilayers of polyatomic materials having different surface and bulk composition. The code includes a variety of models to calculate the elastic and inelastic energy losses during ion slowing down in target materials. The code is highly optimized, fast to run, and easy to use. The agreement between the code and available experimental data is very good.

REFERENCES

1. J. P. BIERSACK and L. G. HAGGMARK, Nucl. Instr. and Meth. 174, 257 (1980).

2. O. S. OEN, D. K. HOLMES, and M. T. ROBINSON, J. Appl. Phys. 34, 302 (1963).

3. T. ISHITANI, R. SHIMIZA, K. MURATA, Jap. J. Appl. Phys, 11, 125 (1972).

4. I. ADESIDA and L. KARAPIPERIS, Rad. Eff. 61, 223 (1982).

5. H. M. ATTAYA, Ph.D. Thesis, University of Wisconsin-Madison, Report, UWFDM-420 (May 1981).

6. A. M. HASSANEIN, "Ion Transport in Materials and Compounds - The ITMC-Code," Argonne National Laboratory, ANL/FPP-TM-199 (1985).

7. J. LINDHARD, V. NIELSON, and M. SCHARFF, Mat. Fys. Medd. Dan. Vid. Selsh. 36, 10 (1968).

8. O. B. FIRSOV, Zb. Eksp. Teor. Fiz. 33, 696 (1957) or Soviet Phys. JETP 6, 534 (1958).

9. K. B. WINTERBON, P. SIGMUND, and J. B. SANDERS, Mat. Fys. Medd. Dan. Vid. Selsk. 37, 14 (1970).

10. P. SIGMUND, Phys. Rev. 184, 383 (1969).

11. K. B. WINTERBON, Rad. Eff. 13, 215 (1972).

12. R. STERNHEIMER, Phys. Rev. 145, 247 (1966).

13. D. K. BRICE, Phys. Rev. 6, 1971 (1972).

14. H. ANDERSON and J. ZIEGLER, "Hydrogen and Helium Stopping Powers and Ranges in All Elements (Pergamon Press, New York, 1977).

15. S. KANG, R. SHIMIZU, and T. OKUTANI, Japanese J. Appl. Phys. 18(9), 1717 (1979).

16. A. SOUTHERN, W. R. WILLIS, M. T. ROBINSON, J. Appl. Phys. 34, 153 (1963.

17. A. R. KRAUSS and D. M. GRUEN, J. Nucl. Mater. 85 & 86, 1179 (1979).

18. A. R. KRAUSS, D. M. GRUEN, and A. B. DEWALD, J. Nucl. Mater., 121, 398 (1984).